Conference paper

Bernd Herzog* and Uli Osterwalder

Simulation of sunscreen performance

DOI 10.1515/pac-2015-0401

Abstract: Sunscreens are used to protect the human skin against harmful effects of solar UV radiation. The most important quantity characterizing sunscreen performance is the sun protection factor (SPF). At the stage of development of new sun protection formulations quick and inexpensive methods for estimation of the UV screening performance are highly desirable. The most convenient approach towards this goal is given by computational simulations. Models for the calculation of the SPF employ the same algorithm as used with in vitro SPF measurements, but replace the transmittance measurement by the calculation of the overall absorbance of the UV filters in an irregular sunscreen film. The simulations require a database with quantitative UV extinction spectra of the relevant UV filters as well as a mathematical description of the film irregularity. The simulation algorithm implies also the consideration of photodegradation properties of the UV filters in the sunscreen composition. Besides using such simulations for designing new sunscreen formulations, the calculations can also support the understanding of sunscreen performance in general.

Keywords: computer simulation; irregular film model; kinetics; Photobiology-16; sun protection factor; sunscreens; UV-visible spectroscopy.

Introduction

It is a well-known fact that an overexposure of human skin by UV light may lead to sunburn and an increased risk for skin cancers [1–3]. With our current knowledge, these effects can be attributed to the UVB part (290–320 nm) as well as to the UVA part (320–400 nm) of the solar spectrum [4]. Accounting for the much higher abundance of UVA in solar radiation compared to UVB, UVA contributes to the development of erythema to about 15 % of the corresponding effect of the overall solar UV radiation. The sun protection factor (SPF) is a measure of how much the erythemally effective radiation is reduced by a sunscreen when applied on human skin. It is defined as the ratio of the minimal erythemal doses (MED) of simulated solar radiation directed to human skin in the presence and in the absence of a sunscreen agent [5]. Based on this definition, in vivo methods for sunscreen testing on volunteers have been established [6–9]. At the time being, such in vivo methods have to be applied before claiming SPF values on sunscreen products.

As testing on volunteers is time-consuming and expensive, for purposes of experimental screening in vitro methods for determination of the SPF have been introduced [10–12]. Such methods are based on measurements of UV transmittance of sunscreen films. Substrates on which the sunscreen films are applied model in some way the inhomogeneous surface structure of the human skin, such as polymethylmethacrylate

Article note: A collection of invited papers based on presentations at the 16th International Congress on Photobiology (ICP-16), Córdoba, Argentina, 7–12 September 2014.

***Corresponding author: Bernd Herzog,** BASF Grenzach GmbH, Koechlinstrasse 1, 79639 Grenzach-Wyhlen, Germany, e-mail: bernd.herzog@basf.com
Uli Osterwalder: BASF Personal Care and Nutrition GmbH, 40789 Monheim, Germany

(PMMA)-plates with rough surface [12]. Measurements of UV transmittance are based on the assumption that the UV-protection of sunscreens is only caused by the attenuation of UV-light. Any other effects, which might be of relevance in vivo, like anti-inflammation or anti-oxidative properties, are not considered.

The sun protection factor is not unequivocally related to the overall UV absorbance spectrum of a sunscreen (absorbance, extinction, and optical density are synonymous terms). That means, it is possible to have quite different levels of UVA protection with the same SPF value. For that reason the protection against UVA has to be assessed with an independent method specific for this spectral range. The most frequently used in vivo method, persistent pigment darkening (PPD), based on the pigmentation of volunteers after irradiation with a pure UVA light source, has been widely taken over by an in vitro method, based on UV transmittance of a sunscreen film and the determination of an UVA protection factor (UVAPF) by adjusting that measurement to the corresponding in vivo SPF [13, 14]. There are several other in vitro methods for the assessment of UVA protection in place [15], all based on measurements of UV transmittance.

Knowing the amounts and characteristics of the UV filter substances of a sunscreen, it is possible to calculate its UV transmittance, when taking also film irregularity and photodegradation kinetics into account. From simulated UV transmittance, SPF and all quantities characterizing protection against UVA can be computed.

Experimental

Some experimental data are necessary for the calculations, such as quantitative UV extinction spectra of the UV absorbers used and the kinetic constants of photodegradation.

For spectroscopic measurements ethanol (p.a., Merck) and bidistilled water were used as solvents. The UV-absorbers used in this work are given below. After the chemical name the INCI name is given in parenthesis followed by the abbreviation and the trade name. The supplier is also indicated. 3-(4-methoxyphenyl)-2-ethylhexyl ester (ethylhexyl methoxycinnamate, EHMC, Uvinul® MC80) from BASF; 2-phenylbenzimidazole-5-sulfonic acid (2-phenylbenzimidazole-5-sulfonic acid, PBSA, Eusolex® 232) from Merck; 2-hydroxy-4-methoxy benzophenone (benzophenone 3, B3, Uvinul® M40) from BASF; titanium dioxide (TiO_2, Eusolex® T2000) from Merck; trianilino-(p-carbo-2′-ethylhexyl-1′-oxi)-1,3,5-triazine (ethylhexyl triazone, EHT, Uvinul® T150) from BASF; 4-t-butyl-4′-methoxydibenzoyl methane (butyl methoxydibenzoyl methane, BMDBM, Parsol® 1789) from DSM; 2-ethylhexyl-2-cyano-3,3-diphenyl-2-propenoate (octocrylene, OCR, Uvinul® N539) from BASF; 2-ethylhexyl p-dimethylaminobenzoate (ethylhexyl dimethyl PABA, OD-PABA, Eusolex® 6007) from Merck; 2,4-bis-{[4-(-2-ethyl-hexyloxi)-2-hydroxy]-phenyl}-6-(4-methoxyphenyl)-(1,3,5)-triazine (bis ethylhexylphenol methoxyphenyl triazine, BEMT, Tinosorb® S) from BASF; 2,2′-Methylene-bis-(6-(2H-benzotriazole-2-yl)-4-(1,1,3,3-tetramethylbutyl)-phenol (Methylene Bis-Benzotriazolyl Tetramethylbutylphenol, MBBT, Tinosorb® M) from BASF; 2-(4-diethylamino-2-hydroxybenzoyl)-benzoic acid hexylester (diethylamino hydroxybenzoyl hexyl benzoate, DHHB, Uvinul® A Plus) from BASF; 2-(2H-benzotriazol-2-yl)-4-methyl-6-[2-methyl-3-[1,3,3,3-tetramethyl-1-[(trimethylsilyl)oxy]disiloxanyl]propyl]-phenol (dromtrizole trisiloxane, DTS, Mexoryl® XL); 3,3′-(1,4-phenylendimethylene)-bis-(7,7-dimethyl-2-oxo-bicyclo-[2.2.1]heptane-1-methane sulfonic acid (terephthalidene dicampher sulfonic acid, TDSA, Mexoryl® SX). The latter two compounds were synthesized at BASF.

UV-spectroscopic transmission measurements were carried out using a Perkin Elmer Lambda 16 spectrometer. UV-transmission spectra of particulate UV-absorbers were recorded with the same instrument using an integration sphere attachment (Labsphere B009-4012). UV-spectra of oil-soluble filters have been measured quantitatively in diluted ethanolic solutions in UV transparent cuvettes of 1 cm optical thickness. UV spectra of the particulate filters MBBT and of TiO_2 were measured quantitatively with dispersions containing the UV-absorber between 0 and 3 % and sandwich-type cuvettes with an optical pathlength of 0.0008 cm [16]. Photodegradation kinetics of single UV filters and also of binary mixtures were measured in sunscreen formulations as reported previously [17, 18].

In vivo SPF data of the sunscreen formulations used in this study were determined according to the International SPF Test Method [8] or the corresponding ISO standard 24444 [9].

Theoretical aspects

Sun protection factors from UV transmittance

The basic principle of sun protection factor calculations is the calculation of the factor by which the intensity of the UV radiation is reduced due to the presence of a sunscreen. This factor is given by the inverse of the UV transmittance of the absorbing film, $1/T$. At a certain wavelength λ, $1/T(\lambda)$ is also designated as monochromatic protection factor (MPF). As the spectral range relevant for the formation of erythema is between 290 and 400 nm, the monochromatic protection factors should be averaged over this range. In order to obtain the SPF, this average must be weighted with the intensity of the light source, $S_s(\lambda)$ and the erythemal action spectrum, $s_{er}(\lambda)$, leading to eq. (1) contributed by Sayre et al. [19]:

$$SPF = \frac{\sum_{290}^{400} s_{er}(\lambda) \cdot S_s(\lambda)}{\sum_{290}^{400} s_{er}(\lambda) \cdot S_s(\lambda) \cdot T(\lambda)} \tag{1}$$

Data for $S_s(\lambda)$ and $s_{er}(\lambda)$ are available [10, 20], but $T(\lambda)$ has to be determined for the respective sunscreen either by in vitro measurement or by calculation. $S_s(\lambda)$ is given in units of W m^{-2} nm^{-1}, $s_{er}(\lambda)$ without units. The product of $S_s(\lambda)$ and $s_{er}(\lambda)$ is called erythemal effectiveness spectrum or erythemally effective irradiance, $E_{er}(\lambda)$, and again has units of W m^{-2} nm^{-1}. The quantities $S_s(\lambda)$ and $s_{er}(\lambda)$ are plotted in Fig. 1. In Fig. 2 the erythemally effective irradiance in the case of no protection, $E_{er}(\lambda)$, is compared to situations of protection, $E_{er}(\lambda) \cdot T(\lambda)$, with sunscreens of SPF = 10 and SPF = 20.

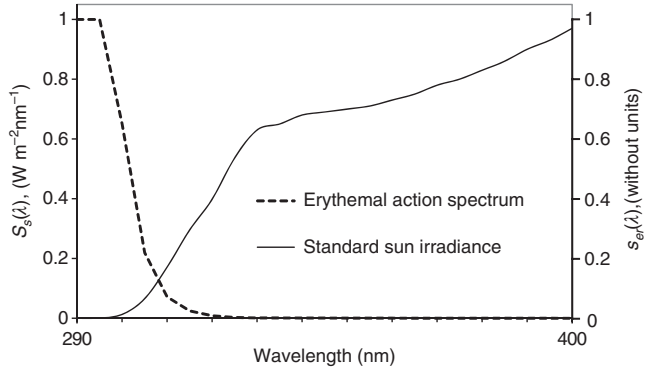

Fig. 1: Erythemal action spectrum and spectrum of standard sun irradiance.

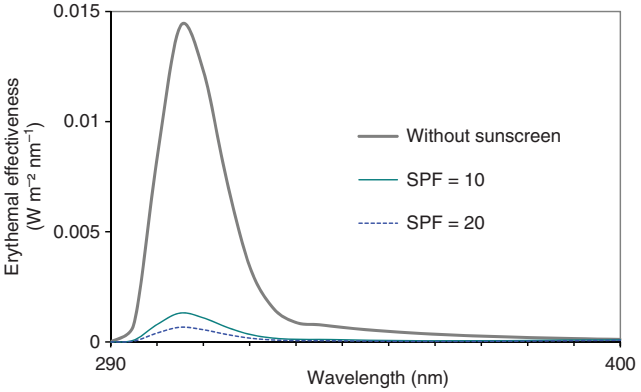

Fig. 2: Erythemal effectiveness in absence and presence of sunscreens.

Overall UV spectrum of a UV filter composition in a sunscreen

Sunscreens in most cases contain more than one UV filter. In order to obtain the overall absorbance of a UV filter composition via Beer-Lambert's law, the overall molar concentration $\bar{c}$ (from the average molecular weight $\bar{M}$) and the average molar extinction coefficient $\bar{\varepsilon}(\lambda)$ are calculated via eq. (2),

$$\bar{M} = \sum_{i=1}^{n} \beta_i \Big/ \sum_{i=1}^{n} \frac{\beta_i}{M_i}, \tag{2a}$$

$$\bar{c} = 10 \cdot \sum_{i=1}^{n} \beta_i / \bar{M}, \tag{2b}$$

$$\bar{\varepsilon}(\lambda) = \sum_{i=1}^{n} \frac{\varepsilon_i(\lambda) \cdot \beta_i}{M_i} \Big/ \sum_{i=1}^{n} \frac{\beta_i}{M_i} \tag{2c}$$

where M_i is the molar mass, β_i the concentration in percent (w/v), and $\varepsilon_i(\lambda)$ the molar extinction coefficient of an individual UV absorber [16, 17].

In order to calculate transmittance via Beer–Lambert's law, the only quantity still missing is the thickness d of the sunscreen film on the skin:

$$T(\lambda) = 10^{-\bar{\varepsilon}(\lambda)\bar{c}d} \tag{3}$$

In the in vivo method for SPF determination, 2 mg/cm² sunscreen are applied on human skin, approximately corresponding to 2 µL/cm². This results in a film of 20 µm (0.002 cm) thickness. However, this film is not homogenous, but irregular. As water evaporates, the film will get thinner, but at the same time the concentrations of the UV-filters will increase accordingly, such that the product $c \cdot d$ will stay constant.

The above calculation of the film thickness is based on the volume of the sunscreen spread on certain skin area. The error made here taking the volume instead of the weight cancels with the error assuming the filter concentrations given in weight per volume, as in practice formulations are prepared in weight per weight.

Accounting for film irregularity

When measuring UV transmittance in vitro, in some way the irregular surface structure of the human skin has to be modeled by using appropriate substrates with rough surface. This is important because the optical transmittance of an absorbing film of uniform thickness always is lower compared to that of a corresponding irregular film of the same average thickness. This fact is illustrated in Fig. 3.

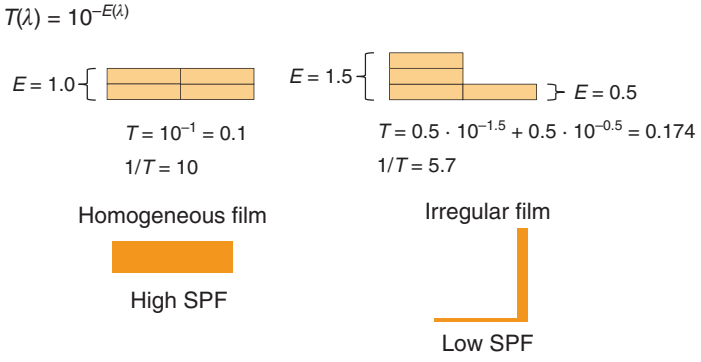

Fig. 3: A homogeneous film always absorbs light better than an irregular film.

The effect can be quite dramatic, and several models describing sunscreen film irregularity have been published [21–24]. The model of Ferrero and coworkers [23], which is employed in the simulations reported here, uses an approach common in surface metrology. In this case, the film profile becomes equivalent to the bearing area curve of Abbot and Firestone [25, 26] and is constructed based on a cumulative distribution function $F(h)$ containing the film height h as a random variable. Among possible probability functions, the authors chose a gamma law representing an asymmetrical distribution, and $f(h)$ is the associated probability density function:

$$f(h) = \left(\frac{h}{b}\right)^{c-1} e^{\left(-\frac{h}{b}\right)} \frac{1}{b\Gamma(c)}, \tag{4}$$

where h is the random variable "relative height," c is the shape parameter to be adjusted, b is needed for normalization and $\Gamma(c)$ is the value of the gamma function at c. The cumulative height distribution $F(h)$ is obtained by integration of $f(h)$ from 0 to ∞:

$$F(h) = \int_0^{\infty} f(h)\,dh. \tag{5}$$

In order to construct the film thickness profile, h is deduced from its cumulative distribution $F(h)$, ranging from 0 to 1. As the area under the film profile is normalized to 1, the following relationship must hold:

$$\int_0^1 h(F)\,dF = 1 \tag{6}$$

The transmittance of the film can then be calculated:

$$T_{\text{film}}(\lambda) = \int_0^1 10^{-\bar{\varepsilon}(\lambda)\bar{c}dh(F)}\,dF \tag{7}$$

The transmittance calculated via eq. (7) can be fed into eq. (1), resulting in an SPF value. The shape parameter c is the screw by which the calculated result can be adjusted to fit the in vivo SPF. In Fig. 4, the density function given in eq. (4) and its cumulative version indicated in eq. (5) are depicted for a shape parameter of c = 1.5. Figure 5 shows the respective film profile defined in eq. (6). In Fig. 6 the influence of the shape parameter is demonstrated for a sunscreen composition with in vivo SPF of 15.5. The larger the shape parameter, the higher the calculated SPF value. Obviously, the value of the SPF is largely determined by the thickness of the thinner parts of the film. In Fig. 5 the film profile of the irregular film is drawn as well as the profile of the corresponding

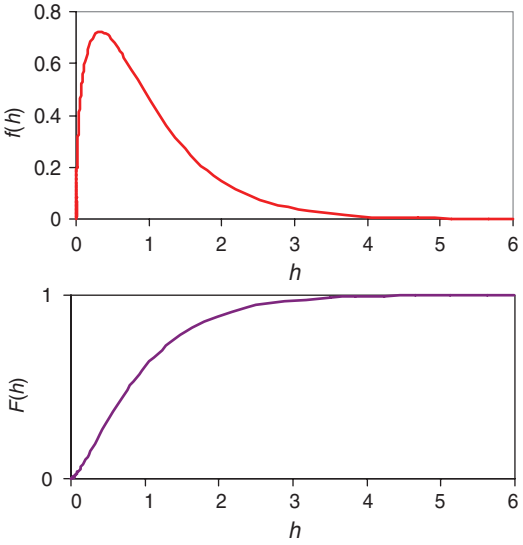

Fig. 4: Probability density distribution $f(h)$ of film thickness h and the corresponding cumulative distribution $F(h)$.

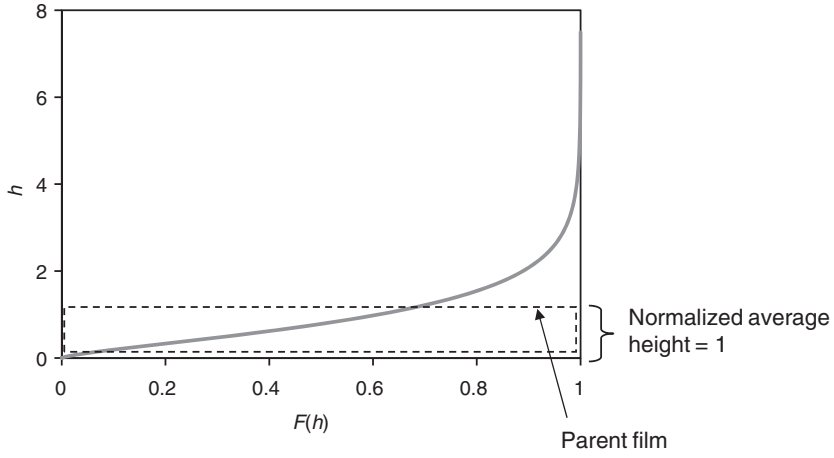

Fig. 5: Construction of irregular film profile by interpreting $F(h)$ as film extension.

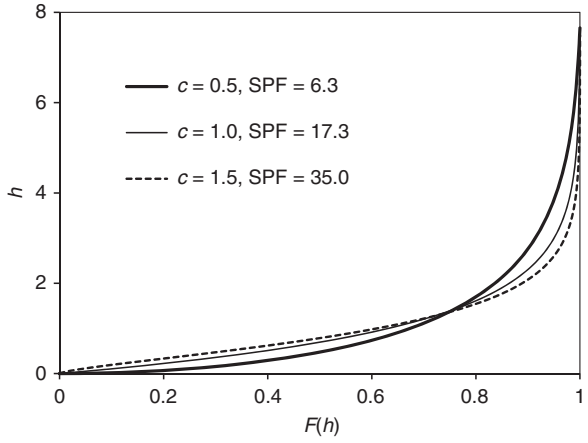

Fig. 6: Structure of irregular film with different values of shape parameter c; corresponding SPF data calculated for the P3 standard sunscreen (composition: 2.78 % PBSA, 3 % EHMC, 0.5 % BMDBM).

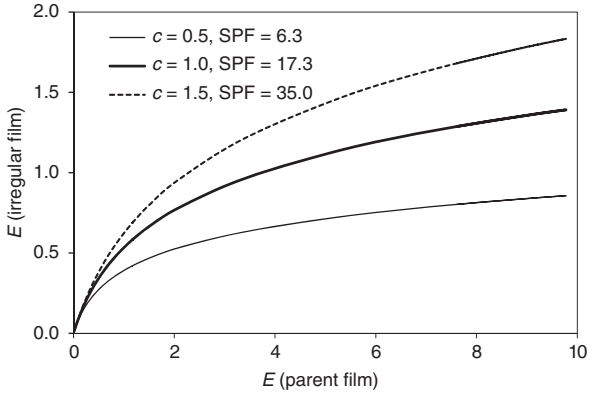

Fig. 7: Absorbance of irregular film as function of parent film absorbance, calculated for P3 standard sunscreen (composition: 2.78 % PBSA, 3 % EHMC, 0.5 % BMDBM) with different values of shape parameter c.

regular film, also called parent film. When plotting the irregular film extinction (E, synonymous with absorbance) against parent film extinction, a non-linear relationship is observed, shown in Fig. 7 for different shape parameters and the composition of the P3 standard formulation [6], but without treatment of photoinstabilities.

Changes of UV transmittance due to photoinstabilities

Equation (1) refers to a static value of the SPF without considering any changes of UV transmittance due to photoinstabilities, which may occur in the course of the irradiation process involved with SPF determination in vivo. In order to take this into account when performing in vitro SPF measurements, eq. (1) was modified by Stanfield et al. [27], with t_{MED} referring to the time, after which one minimal erythemal dose (1 MED) is transmitted through the sunscreen film:

$$SPF = \frac{\sum_0^{t_{MED}} \sum_{290}^{400} s_{er}(\lambda) \cdot S_s(\lambda)}{\sum_0^{t_{MED}} \sum_{290}^{400} s_{er}(\lambda) \cdot S_s(\lambda) \cdot T(t,\lambda)} \tag{8}$$

This approach mimics the conditions of SPF determination in vivo. A similar and equivalent method was described by Wloka et al. [28]. These procedures were developed for in vitro SPF measurements, but can equally be applied when UV transmittance is calculated, under the prerequisite that decay constants of the photodegradation of the UV filters are known [17, 18]. The kinetics of UV filter photodegradation is approximated with a first-order law, where c_i is the molar concentration of UV filter i ($c_{i,0}$ without irradiation, $c_{i,\mathrm{UVdose}}$ after irradiation with a certain UV dose), and k_i is its kinetic constant of photodegradation:

$$c_{i,\mathrm{UV\ dose}} = c_{i,0} \cdot \exp(-k_i \cdot UV\ dose) \tag{9}$$

For practical reasons, instead of time, UV dose is written in eq. (9), which is proportional to irradiation time. There can be stabilizing or destabilizing interactions between different UV filters. This is accounted for by formalisms which decrease the k_i in case of stabilization and increase them in case of destabilization. For stabilization the following equation was found [18]:

$$k_{i,j} = (1/k_{i,0} + q_j\beta_j)^{-1}, \tag{10},$$

where $k_{i,0}$ is the degradation constant without stabilization, q_j is the stabilizer constant of stabilizer j, and β_j is its concentration in percent (w/v). For destabilization eq. (11) is employed:

$$k_{i,m} = k_{i,0}(1 + r_m\beta_m), \tag{11}$$

where $k_{i,0}$ is the degradation constant without destabilization, r_m is the destabilization constant of destabilizer m, and β_m is its concentration in percent (w/v). In Table 1 values of k_i are given for the UV filters used in this work. Table 2 lists stabilization and destabilization constants. By determining the interaction factors $k_{i,j}/k_{i,0}$ and $k_{i,m}/k_{i,0}$, any number of interactions can be taken into account by multiplying $k_{i,0}$ with all existing interaction factors.

Table 1: Photodegradation constants of UV filters used in this work.

UV filter	Photodegradation constant k_i (MED^{-1})
OCR	0.0010
PBSA	0.0047
EHT	0.0058
OD-PABA	0.0139
EHMC	0.0417
B3	0.0010
DTS	0.0010
BEMT	0.0010
MBBT	0.0002
DHHB	0.0021
TDSA	0.0058
BMDBM	0.2200

Table 2: Stabilizing constants q_j and destabilizing constants r_m.

UV filter combination (the second filter is the stabilizer or destabilizer)	Stabilizing constants q_j (MED · %$^{-1}$)	Destabilizing constants r_m (%$^{-1}$)
BMDBM + OCR	2.33	
BMDBM + BEMT	0.90	
EHMC + OCR	2.33	
EHMC + BEMT	0.90	
EHMC + MBBT	0.90	
EHMC + BMDBM		0.244
BMDBM + EHMC		0.012

In addition, the photostability of photounstable UV filters can be improved when UV light is strongly absorbed in their environment. The following relationship was established empirically in order to implement this effect:

$$k_{i,OD} = \left(\frac{OI_i}{OI_{sf}} \right)^{0.8304}, \tag{12}$$

where OI_i = overlap integral of the absorbance spectrum of 2 % (w/v) of the respective UV filter at an optical thickness of d = 0.002 cm and the irradiance spectrum of the lamp used for the photostability assessment [29], and OI_{sf} = overlap integral of the absorbance spectrum of the irregular sunscreen film and the irradiance spectrum of the lamp used for photostability measurements. If $k_{i,OD} < 1$, there is a protective effect due to the overall optical density. Only then $k_{i,OD}$ is considered by multiplying it with the decay constant of the respective filter.

For the SPF calculation with consideration of photoinstabilities the approach of Wloka et al. [28] is used. For that purpose UV dose dependent concentrations of the UV filters are calculated using eq. (9) and with that, UV dose dependent SPF values. The inverse of the UV dose-dependent SPF is plotted against the irradiation dose given in minimal erythemal doses (MEDs). The area under the curve can be interpreted as the erythemally effective irradiation dose. When this area becomes unity, 1 MED has been transmitted through the sunscreen film, what exactly corresponds to the principle of the in vivo SPF measurement. Thus the SPF can be read at this point from the respective UV-dose given on the abscissa. An example with a resulting SPF of 10 is shown in Fig. 8.

With photounstable UV filters, the spectrum of the absorbance of the sunscreen film varies with time. According to Stanfield et al. [27] it is possible to determine the effective UV absorbance spectrum, regarding the period from beginning of irradiation up to the point where 1 MED is transmitted. To this end, the transmitted UV-doses with (D_p) and without protection (D_u) are integrated over time, and transmittance, now called integrated transmittance, is calculated for each wavelength λ:

$$T_{\text{int}}(\lambda) = D_p(\lambda) / D_u(\lambda), \tag{13}$$

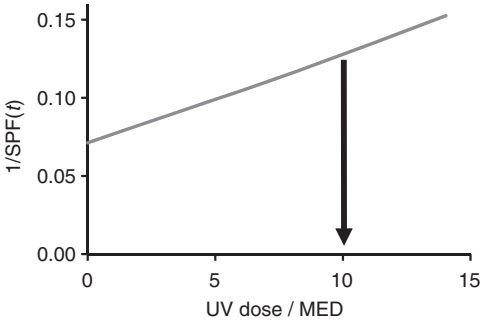

Fig. 8: Evaluation of the calculated SPF with photounstable sunscreens.

where

$$D_u = \int_0^{t_{MED}} S_s(\lambda)\,dt \tag{14}$$

and

$$D_p = \int_0^{t_{MED}} S_s(\lambda) \cdot T(\lambda,t)\,dt. \tag{15}$$

The integrated absorbance can then be obtained from integrated transmittance:

$$E_{int}(\lambda) = \lg(1/T_{int}(\lambda)). \tag{16}$$

Figure 9 illustrates the concept of integrated transmittance and absorbance with an example of a photounstable composition (5 % EHMC, 4 % BMDBM, 3 % OCR) with calculated SPF of 17.5.

Calibration of the model

As already mentioned, the screw by which the calculated SPF can be adjusted to SPF in vivo data is the shape parameter in eq. (4). At first sight, the model has only this single parameter. However, it is not possible to get satisfactory correlation with compositions covering a brought range of sun protection factors using just one value of the shape parameter. So the shape parameter has to vary as function of the filter composition, and there are two observations indicating, how this could be explained: First, presence of a higher amount of emollient leads to an increase of the SPF at constant filter composition, and second, there is a synergistic effect on the SPF when sunscreens contain water- and oil-soluble UV filters rather than having the UV filters only in one phase of the preparation. As the only input for the calculations is the UV filter composition, the first point can be handled by scaling the shape parameter with the overall filter concentration (OFC) which for most sunscreen compositions is an indicator of the amount of oil used. The overall UV filter concentration for filters *i* to *n* is given as:

$$OFC = \sum_i^n \beta_i \tag{17}$$

For the second point, a relevant parameter is the relative erythema active extinction in the oil phase, REAE. For a single filter *i* with concentration β_i the erythema active extinction EAE_i is calculated via eq. (18):

$$EAE_i = \beta_i \cdot \sum_{\lambda=290}^{400} E_{11}(i,\lambda) \cdot s_{er}(\lambda) \cdot S_s(\lambda) \tag{18}$$

where $E_{11}(i,\lambda)$ is the specific extinction of filter *i* at wavelength λ, the other quantities have the same meaning as in eqs. (1) and (2). The relative erythema active extinction in the oil phase is given via eq. (19):

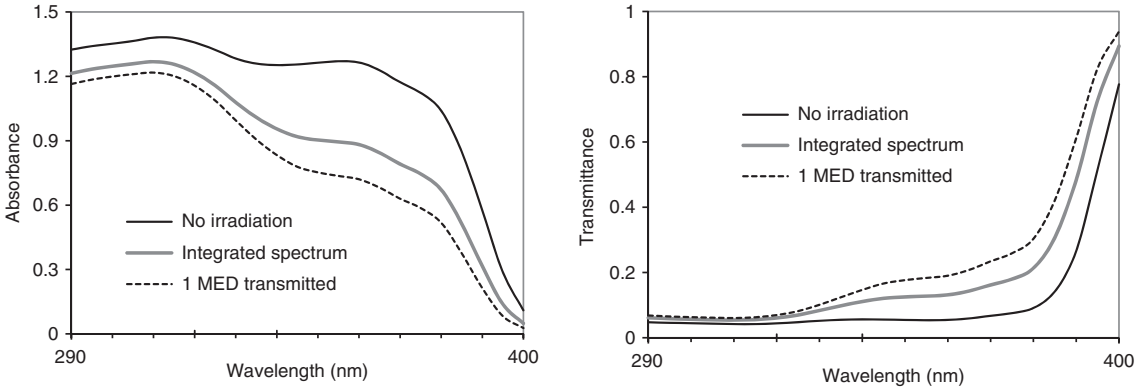

Fig. 9: Integrated spectra calculated for a sunscreen composition of 5 % EHMC, 4 % BMDBM, and 3 % OCR.

$$REAE = \sum_i EAE_i(o) / [\sum_i EAE_i(o) + \sum_k EAE_k(w)], \tag{19}$$

where $EAE_k(w)$ is the erythema active extinction of filter k in the water-phase. For the variation of the shape parameter as function of filter composition, the following function has been found:

$$c = p1 + p2 \cdot [\mathrm{OFC}^{p3} / (\mathrm{OFC}^{p3} + p4)] + p5/4 + p5 \cdot (\mathrm{REAE} - 0.5)^2 \tag{20}$$

The values of the parameters have been adjusted to $p1 = 0.33$, $p2 = 0.69$, $p3 = 0.89$, $p4 = 1.95$, and $p5 = 0.5$. Thus, the distribution of the UV filters in the water and the oil phase is taken into account as well as the overall filter content, which in a way can be interpreted as formulation influences.

The calibration of the parameters in eq. (20) was achieved by using in vivo data of ring tests where several laboratories had been involved, or our own data, where in vivo studies had been repeated several times on the same sunscreen formulations (P1, P2 and P3 [6], S2 [30, 31], S1, C1, C2 and P4 [17, 32]). Table 3 lists the UV filter compositions and corresponding data, and the correlation of simulated and in vivo data is shown in Fig. 10. The slope of the correlation is 1.015 and the correlation coefficient is $r^2 = 0.9423$.

Protection against UVA radiation

The in vivo method used for UVA protection assessment is persistent pigment darkening (PPD). PPD is the official method for assessment of the UVA-protection in Japan [32]. In analogy to the erythemal response

Table 3: Calibration of the model parameters using sunscreens with in vivo data based on large sample sizes [6, 17, 30–32]; in vivo data given with confidence intervals based on 95 % level of significance.

Sunscreen	Filter composition	SPF in vivo	Calculated SPF
P1	2.7 % EHMC	4.2 ± 0.2	5.1
P2	7 % OD-PABA, 3 % B-3	12.7 ± 1.2	16.7
P3	2.78 % PBSA, 3 % EHMC, 0.5 % BMDBM	15.5 ± 1.5	12.1
S1	3 % EHMC, 5 % BMDBM	8.2 ± 0.8	9.8
S2	3 % EHMC, 5 % BMDBM, 3 % OCR, 2 % BEMT	16.0 ± 2.7	20.2
C1	3 % BEMT	7.7 ± 0.8	7.3
C2	2 % BEMT, 4 % MBBT, 5 % EHMC	29.0 ± 5.0	27.2
P4	10 % MBBT, 5 % EHMC	35.7 ± 3.2	36.2

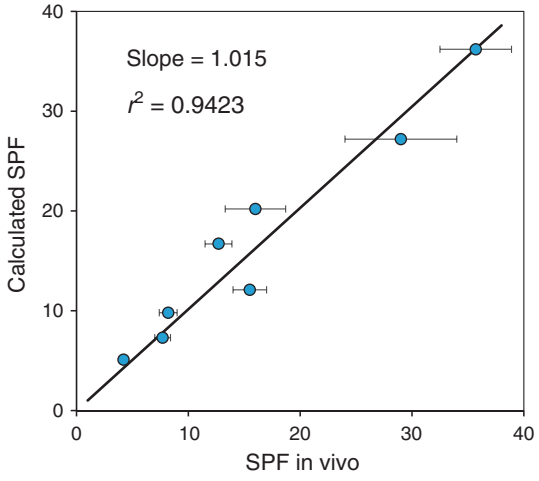

Fig. 10: Correlation of calculated SPF and in vivo SPF of formulations used for calibration of the model parameters (data in Table 3).

expressed by the SPF, the UVA-protection factor (UVAPF) values are determined by the biological endpoint of spontaneous pigmentation after irradiation with a UVA light source.

The UVAPF is simulated in a similar way like the SPF from calculated transmittance $T(\lambda)$ taking photodegradation of the filter molecules into account, but now employing the spectrum of an UVA lamp, $S_{UVA}(\lambda)$, and the PPD action spectrum $s_{PPD}(\lambda)$ in eq. (8), and the time t_{MPD} after which a minimal pigmenting dose (1 MPD) is transmitted:

$$UVAPF = \frac{\sum_0^{t_{MPD}} \sum_{320}^{400} s_{PPD}(\lambda) \cdot S_{UVA}(\lambda)}{\sum_0^{t_{MPD}} \sum_{320}^{400} s_{PPD}(\lambda) \cdot S_{UVA}(\lambda) \cdot T(t,\lambda)} \tag{21}$$

For the calculation of UV transmittance in eq. (21), the same principles are applied as previously described for the calculation of the SPF. However, the overall UV dose needed to achieve 1 MPD is higher than that to achieve 1 MED. Thus, irradiation time with PPD experiments is about five times longer. Considering that the UVB is filtered off, still a factor 3.2 has to be taken into account for the calculation of UV filter photodegradation.

An in vitro method for determination of the UVA-PF has been developed [13] and is meanwhile standardized [14]. In order to simulate this method, the film irregularity model is not used, but a relationship between parent film extinction and extinction of the film on the substrate, based on in vitro data, leading to similar curves as shown in Fig. 7:

$$E_{\text{in vitro}} = a \cdot E_{\text{parent}}^{b} \tag{22}$$

Assuming the thickness of the homogenous parent film to be 0.00075 cm, the parameters were determined to $a = 0.5072$ and $b = 0.5466$. In that way in vitro extinction and transmittance spectra are obtained resulting in a simulated in vitro SPF, the value of which may differ from the simulated in vivo SPF. The corresponding simulated in vitro transmission spectrum is then transformed, such that the simulated in vitro SPF matches the simulated in vivo SPF. This is achieved by adjusting a parameter C as an exponent to the transmittance $T(\lambda)$:

$$UVAPF_{in\ vitro} = \frac{\sum_{320}^{400} s_{PPD}(\lambda) \cdot S_{UVA}(\lambda)}{\sum_{320}^{400} s_{PPD}(\lambda) \cdot S_{UVA}(\lambda) \cdot T(\lambda)^{C}} \tag{23}$$

The irradiation step involved in this method [14], which scales with the UVAPF obtained without irradiation, is also taken into account.

Other quantities characterizing the UVA protection such as UVA/UVB-ratio, critical wavelength and others [15] can also be deduced from the calculated absorbance or transmittance spectra. The UVA/UVB-ratio is the average absorbance in the UVA-range divided by the average absorbance in the UVB-range. The critical wavelength (λ_c) is given as the wavelength at which 90 % of the total area under the absorbance curve is achieved.

Simulation examples

Variation of application amount

The question how the sun protection factor depends on application amount is of interest, since people tend to apply much less sunscreen as is used in the in vivo SPF test performed on volunteers. A multi-center study showed, that there is a linear dependence of the SPF on application amount [33], although some authors claim an exponential relationship [34]. From eq. (1) it can be deduced that an exponential relationship can only be expected if the transmittance would be approximately the same at all wavelength between 290 and 400 nm. As there is also significant erythemal efficacy in the UVA range, the SPF of a pure UVB sunscreen will even show saturation-like behavior when its application amount is increased.

Figures 11 and 12 show calculations for two extreme examples, comparing a broad-spectrum sunscreen (5 % BEMT and 5 % MBBT, UVA/UVB-ratio = 0.92) and a sunscreen containing only UVB filters (5 % EHT and 5 % PBSA) UVA/UVB-ratio = 0.16), both with overall filter concentrations of 10 %. Indeed, the SPF of the broad-spectrum composition shows slightly exponential behavior, whereas that of the UVB sunscreen approaches saturation when the application amount is increased.

In [33] three sunscreen products were investigated in a ring study. All products showed linear dependence of the SPF on application amount. In order to simulate the behavior of these products, the filter contents of products B and C were analyzed. Product B with label SPF 20 contained 10 % OCR, 2.7 % BMDBM, 1.8 % TiO_2, 1.0 % DTS, 1.0 % EHT, and 0.5 % TDSA (abbreviations are explained in the experimental section). Product C with label SPF 25 contained 4.2 % EHT, 3.5 % TiO_2, and 2.0 % BEMT. Knowing the UV filter concentrations it is possible to calculate the SPF as function of application amount. The simulations shown in Fig. 13 are in good agreement with the experimental data [33] and also represent approximately the linear dependence of the SPF on application amount. The UVA/UVB-ratios are in between those of the extreme examples shown in Fig. 12 (0.72 for product B, and 0.53 for product C).

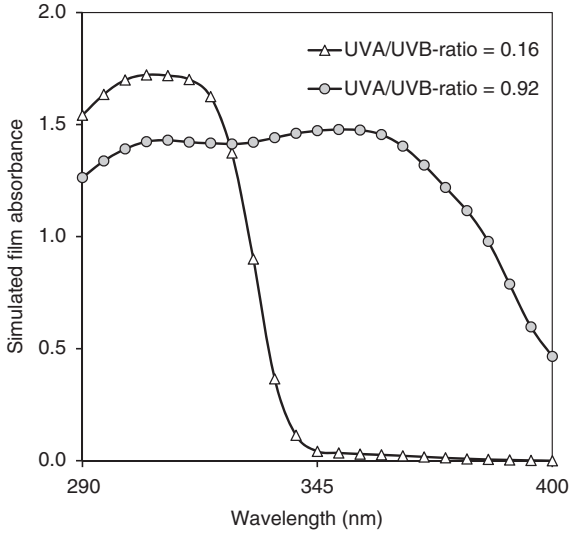

Fig. 11: Calculated sunscreen spectra of irregular films of composition 5 % EHT + 5 % PBSA (UVA/UVB-ratio = 0.16) and 5 % BEMT + 5 % MBBT (UVA/UVB-ratio = 0.92).

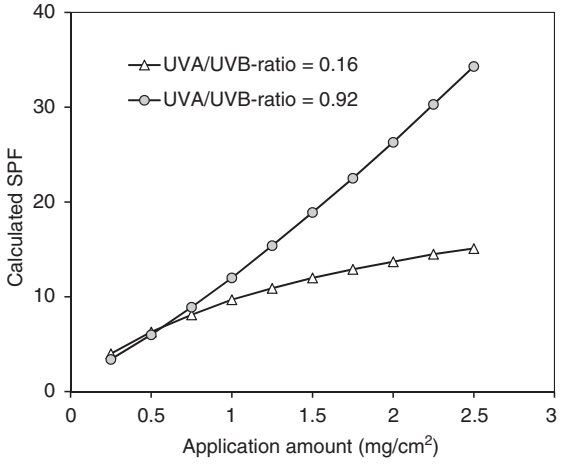

Fig. 12: Calculated SPF as function of application amount for two sunscreens with different UVA/UVB-ratios (0.16 and 0.92).

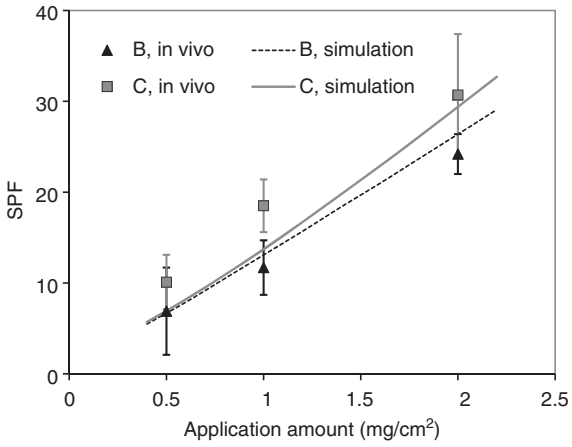

Fig. 13: SPF as function of application amount for two sunscreens investigated in reference [33].

Variation of light source spectrum

For determination of SPF in vivo, a light source is used with a spectrum deviating in the UVA-I range strongly from solar spectra, as the visible light is filtered off. The question how much this affects the protection under natural solar conditions, has already been addressed in an experimental study [35]. It was observed that the SPF is lowered by about one third when UVA-I is not filtered. It was also demonstrated, that with different types of solar simulators, SPF results may vary by more than a factor of two [36]. Figure 14 shows a comparison of a standard solar spectrum [10], the spectrum defined in the International SPF method [8] and the latter one multiplied with the transmission spectrum of the WG335 filter [37].

In Fig. 11 the irregular film absorbances of two quite different UV filter compositions are shown for the usual application amount of 2 mg/cm². Considering the SPF of the two compositions, the case with UVA/UVB-ratio = 0.16 gives an SPF of 13.7 when calculated with the laboratory light source spectrum. Taking the spectrum of the standard sun, the SPF is only 10.6, about 23 % lower. In comparison, the SPF of the composition with UVA/UVB-ratio = 0.92 is 26.3 with the laboratory lamp and 25.0 when taking the standard sun spectrum, which is only 5 % lower. That means, the more uniform a sunscreen absorbs in the UVB and the UVA range, the less its performance will depend on the spectrum of the light source.

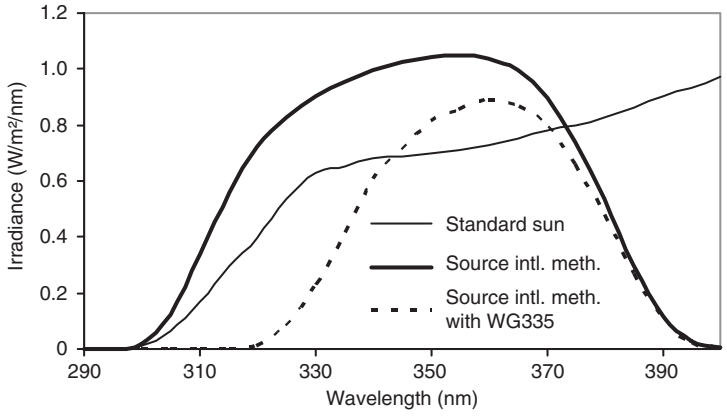

Fig. 14: Different light source spectra.

Table 4: Correlation of in vivo and calculated SPF of formulations using a UV filter concentrate [39, 40]; in vivo data given with confidence intervals based on 95 % level of significance.

% Premix	Filter composition	SPF in vivo	Calculated SPF
6	1.2 % EHMC, 1.2 % DHHB, 0.36 % EHT, 0.3 % BEMT	6.5 ± 2.5	6.1
10	2 % EHMC, 2 % DHHB, 0.6 % EHT, 0.5 % BEMT	10.0 ± 2.6	9.8
15	3 % EHMC, 3 % DHHB, 0.9 % EHT, 0.75 % BEMT	17.6 ± 5.0	14.8
20	4 % EHMC, 4 % DHHB, 1.2 % EHT, 1 % BEMT	20.9 ± 4.8	19.8
25	5 % EHMC, 5 % DHHB, 1.5 % EHT, 1.25 % BEMT	30.4 ± 3.8	25.0
30	6 % EHMC, 6 % DHHB, 1.8 % EHT, 1.5 % BEMT	35.0 ± 5.3	30.2
50	10 % EHMC, 10 % DHHB, 3 % EHT, 2.5 % BEMT	48.8 ± 4.9	51.0

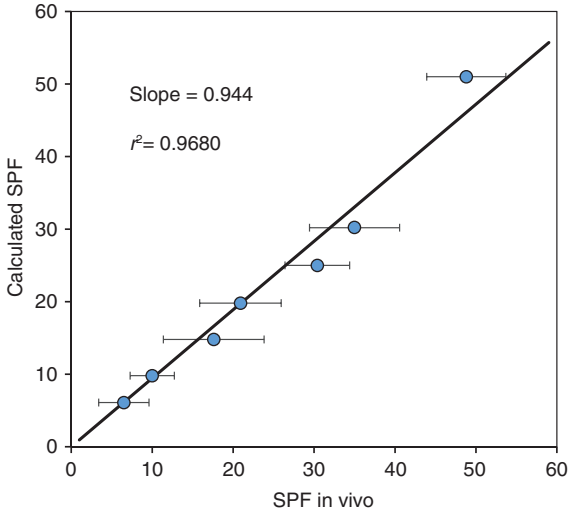

Fig. 15: Correlation of calculated SPF and in vivo SPF of formulations based on a UV filter concentrate (data in Table 4).

Development of new sunscreens

The sunscreen simulator model described here [38] is widely used in the cosmetic industry for the design of new sunscreen formulations. An example where it has been successfully applied was the development of a premix concept for a simple preparation procedure of sunscreens [39, 40]. The concentrate consists of a mixture of four UV absorbers, 20 % EHMC, 20 % DHHB, 6 % EHT, and 5 % BEMT, and cosmetic oils and emulsifiers added to 100 %. Upon dilution with water an emulsion forms spontaneously. In that way sunscreen formulations can be easily prepared. With the chosen filter composition the resulting emulsions comply with the requirements for UVA protection, such as UVAPF/SPF ≥ 1/3 and $\lambda_c \geq 370$ nm. In Table 4 filter concentrations, in vivo SPF and calculated SPF data are given for different dilutions of the concentrate. The correlation is shown in Fig. 15. The model prediction of the SPF (slope = 0.944) and the correlation of in vivo and simulated SPF data ($r^2 = 0.9680$) are excellent.

Conclusion

For the simulation of sunscreen performance the following elements are needed: a database with quantitative UV spectra of the relevant UV filters, a mathematical description of the irregularity profile of the sunscreen film on the skin, and the consideration of changes in UV filter concentration due to photoinstabilities.

Such simulations can significantly reduce the amount of experimental work needed when developing new sunscreen formulations, and additionally help understanding how sunscreens work when simulating their behavior under different conditions [41].

References

[1] F. R. de Gruijl. *Skin Pharmacol. Appl. Skin Physiol*. **15**, 316 (2002).
[2] H. N. Ananthaswamy, S. M. Loughlin, S. E. Ulrich, M. L. Kripke. *J. Invest. Dermatol. Symp. Proc.* **3**, 52 (1998).
[3] F. R. de Gruijl, H. J. C. M. Sterenborg, P. D. Forbes, R. E. Davies, C. Cole, G. Kelfkens, H. van Weelden, H. Slaper, J. C. van der Leun. *Cancer Res.* **53**, 53 (1993).
[4] S. Seité, D. Moyal, M. P. Verdie, C. Hourseau, A. Fourtanier. *Photodermatol. Photoimmunol. Photomed.* **16**, 3 (2000).
[5] R. Schulze. *Parfüm. Kosmet.* **37**, 6, 7, 310, 365 (1956).
[6] J. Ferguson, M. Brown, D. Alert, S. Bielfeldt, J. Brown, A. Chardon, C. Hourseau, C. Mazilier, J. Cuthbert, D. Arcy-Burt, J. Jolley, M. Murdoch, P. Finkel, P. Masson, F. Merot, A. Maclennon, J. Poret, S. Siladji. *Int. J. Cosmet. Sci.* **18**, 203 (1996).
[7] Food and Drug Administration, FDA, USA. Labeling and effectiveness testing; sunscreen drug products for over-the-counter human use, final rule. Fed. Reg. 76/117, 35620 (2011).
[8] International sun protection factor (SPF) test method CFFA SA, COLIPA, JCIA, CTFA, (2006).
[9] ISO 24444:2010. In vivo determination of the sun protection factor (SPF).
[10] B. L. Diffey, J. Robson. *J. Soc. Cosmet. Chem.* **40**, 127 (1989).
[11] H. Tronnier, D. Kockott, B. Meick, N. Hani, U. Heinrich. *Parfüm. Kosmet.* **77**, 326 (1996).
[12] S. Miksa, D. Lutz, C. Guy. *Cosmet. Toiletries* **129**, 30 (2014).
[13] COLIPA method for the in vitro protection of UVA protection provided by sunscreen products. The European Cosmetics Toiletry and Perfumery Association – COLIPA (now: *Cosmetics Europe*), Rue de la Loi 223/2, B-1040 Bruxelles (2007).
[14] ISO 24443:2012. Determination of sunscreen UVA photoprotection in vitro.
[15] B. L. Diffey. *Int. J. Cosmet. Sci.* **16**, 47 (1994).
[16] B. Herzog. *J. Cosmet. Sci.* **53**, 11 (2002).
[17] B. Herzog, S. Mongiat, K. Quass, C. Deshayes. *J. Pharm. Sci.* **93**, 1780 (2004).
[18] B. Herzog, M. Wehrle, K. Quass. *Photochemistry and Photobiology, Symposium in Print: Pharmaceutical Photochemistry* 85, 869–878 (2009).
[19] R. M. Sayre, P. P. Agin, G. J. LeVee, E. Marlowe. *Photochem. Photobiol.* **29**, 559 (1979).
[20] A. F. McKinlay, B. L. Diffey. *CIE J.* **6**, 17 (1987).
[21] J. J. O'Neill. *J. Pharm. Sci.* **73**, 888 (1984).
[22] B. Herzog, in *Sunscreens – Regulation and Commercial Development*, Nadim Shaath (Ed.), 3rd ed., p. 881, Taylor & Francis, Boca Raton (2005).
[23] L. Ferrero, M. Pissavini, S. Marguerie, L. Zastrow. *J. Cosmet. Sci.* **54**, 63 (2003).
[24] B. Herzog, in *Colloids in Cosmetics and Personal Care*, TF Tadros (Ed.), vol. 4, p. 275, Wiley VCH, Weinheim (2008).
[25] R. T. Thomas, in *Rough Surfaces*, 2nd ed., p. 91, Imperial College Press (1998).
[26] E. P. Abbott, F. A. Fireston. *Mech. Eng.* **55**, 569 (1933).
[27] J. Stanfield, U. Osterwalder, B. Herzog. *Photochem. Photobiol. Sci.* **9**, 489 (2010).
[28] M. Wloka, R. F. M. Lange, H. Flösser-Müller. Proc. Int. Sun Protection Conference, London (2005).
[29] B. Herzog, S. Müller, M. Sohn, U. Osterwalder. *SOFW J.* **133**, 26 (2007).
[30] D. Moyal, M. Pissavini, F. Boyer, V. Perier, J. H. Frelon. *Int. J. Cosmet. Sci.* **29**, 443 (2007).
[31] The in vivo SPF of the S2 standard sunscreen was provided by D. Moyal, L'Oreal Recherche.
[32] JCIA Measurement Standard for UVA Protection Efficacy. Japan Cosmetic Industry Association – JCIA, 9-14, Toranomon 2-Chome, Minato-Ku Tokyo, p. 105 (1995).
[33] R. Bimczok, H. Gers-Barlag, C. Mundt, E. Klette, S. Bielfeldt, T. Rudolph, F. Pflücker, U. Heinrich, H. Tronnier, W. Johncock, B. Klebon, H. Westenfelder, H. Flößer-Müller, K. Jenni, D. Kockott, J. Lademann, B. Herzog, M. Rohr. *Skin Pharmacol. Physiol.* **20**, 57 (2007).
[34] N. Bech-Thomsen, H. C. Wulf. *Photodermatol. Photoimmunol. Photomed.* **9**, 242 (1993).
[35] R. M. Sayre, J. Stanfield, A. J. Bush, D. L. Lott. *Photodermatol. Photoimmunol. Photomed.* **17**, 278 (2001).
[36] B. Uhlmann, T. Mann, H. Gers-Barlag, D. Alert, G. Sauermann. *Int. J. Cosmet. Sci.* **18**, 13 (1996).
[37] http:\\www.uqgoptics.com/materials_filters_schott_colourless_WG335.spx. Accessed 31 August 2015.
[38] BASF sunscreen simulator, BASF SE, Ludwigshafen, Germany. 2010. Available at http://www.basf.com/sunscreen-simulator.
[39] S. Acker, M. Hloucha, U. Osterwalder. *SOFW J.* **40**, 24 (2014).
[40] S. Acker, M. Hloucha, U. Osterwalder. *Global Ingredients and Formulation Guide*, SOFW, p. 152 (2014).
[41] D. J. McGarvey. *Educ. Chem.* **44**, 116 (2007).